Supplementary information

Aluminum-Electrode-Based Electrocoagulation for Efficient Pb^{2+} ions and TOC Removal from Industrial Effluent: Performance to Techno-Economic Analysis

Gowthaman Somasundaram and Selvaraju Thangavelu*

Department of Chemistry, Bharathiar University, Coimbatore-641 046.

Email: veluselvaraju@gmail.com; selvaraju@buc.edu.in

S1. ECP removal mechanism

The mechanistic model was developed within the reaction in the ECP as irreversible and follows the subsequent chemical reactions as shown in **Eqns. (S1-S3)**. Initially, the oxidation reaction produces Al^{3+} ions at the anode during the ECP, depicted by **Eqn. (S1).**

Oxidation at the anode,

$$Al_{(s)} \rightarrow Al^{3+}_{(aq)} + 3e^- \quad \textbf{(S1)}$$

Reduction at the cathode,

Meanwhile, Al^{3+} ions contribute to charge neutralization to form $Al(OH)_3$, and water undergoes a reduction reaction at the cathode, producing OH^- ions and H_2 gas **(Eqn.(S2)).**

$$3H_2O_{(l)} + 3e^- \rightarrow \frac{3}{2}H_{2(g)} + 3OH^-_{(aq)} \quad \textbf{(S2)}$$

As a result of a bulk chemical reaction, $Al(OH)_{3(s)}$ is produced and mediates to generate metallic coagulants **(Eqn.(S3)).**

$$Al^{3+}_{(aq)} + 3H_2O_{(l)(aq)} \rightarrow Al(OH)_{3(s)}\downarrow + \frac{3}{2}H_{2(g)} \quad \textbf{(S3)}$$

SI2. Analytical techniques

ECP was carried out using a DC power supply (Aplab high-voltage DC H1010, Chennai, INDIA), with the respective electrode terminals connected via Cu wires. The final voltage was measured using a multimeter (Digital multimeter HTC830^{+}), and the pH was measured using a pH meter (EUTECH-instruments multi-parameter PCSTestr ^{TM}35, China). The surface morphologies of pre- and post-treatment of the Al electrode were determined using Field Emission scanning electron microscopy (FE-SEM) coupled with energy-dispersive X-ray spectroscopy (EDAX) (TESCAN FE-SEM VEGA 3, USA). An X-ray diffractometer (XRD) was used to examine the crystallinity of pre- and post-Al electrodes (Shimadzu XRD-6000, Japan). UV-Vis spectroscopy (Shimadzu UV-2700 with ISR-2600 plus) was used for analyzing the absorbance characteristics of industrial effluent before and after ECP treatment. TOC in the industrial effluent was quantified using a TOC analyzer (Analytik Jena multi-N/C 3100, Germany). Elemental concentrations were determined via atomic absorption spectroscopy (AAS) (AAS-263, Systronics, India). The FT-IR spectrometer (Bruker TENSOR 27) was used to identify the major functional groups, and X-ray photoelectron spectroscopy (XPS, ESCALAB 250XI, Germany) was used to characterize the chemical states of the elements present in the sludge. AFM studies (Park NX10, Japan) were performed to analyze the surface topography of the anode and cathode by scanning to display any solid deposition (fouling) and pit progress (corrosion). All electrochemical tests were conducted using an Autolab multichannel potentiostat/galvanostat electrochemical workstation (AUT.MAC204.S, Netherlands).

Table S1 Characteristics of the initial assessment of textile effluent.

Parameters	Values	units
pH	6.2	-
TOC	307.8	mg/L
TC	1050	mg/L
IC	1360	mg/L
Pb (lead)	520	mg/L
Colour	Reddish brown	-

SI3. Set-up of laboratory-batch study for electrocoagulation treatment process

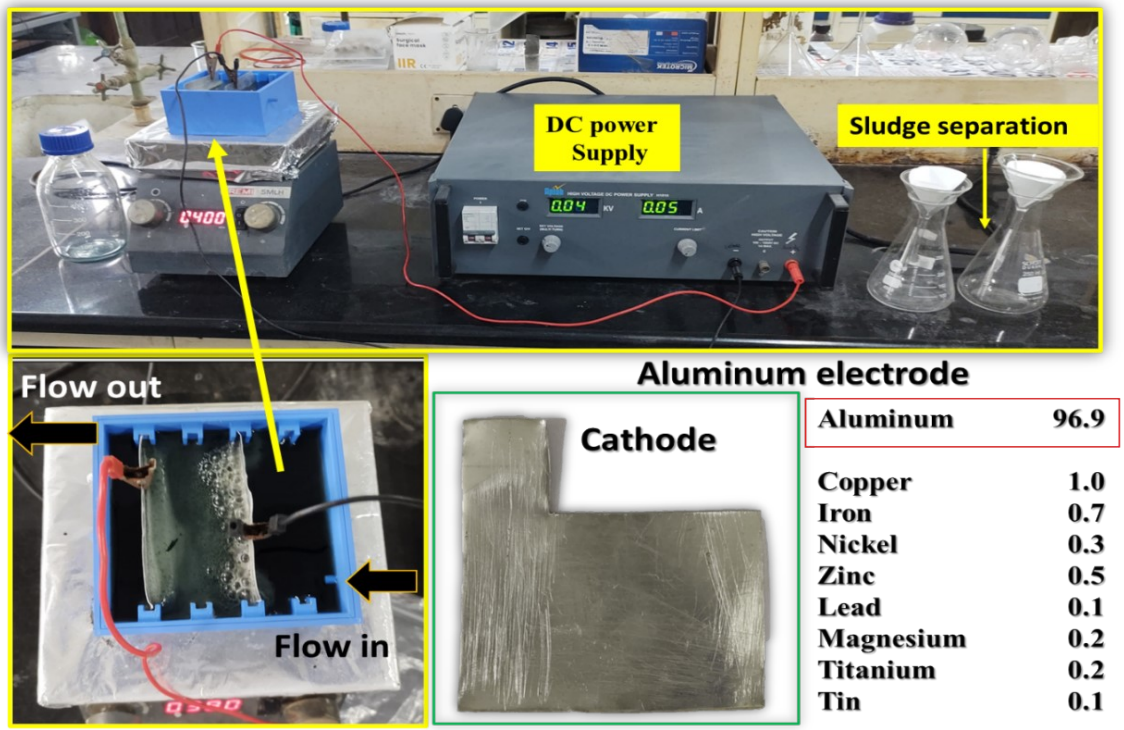

Fig. S1 Continuous flow through ECP with an EC cell. The photo on the bottom (left) shows a 1-liter lab-scale batch reactor. The photo on the right (bottom) with a table shows the properties of the Al electrode.

The lab-batch reactor was conducted in a 1.5 L 3D plastic chamber as described in a schematic DC-based ECP shown in **Fig. S1**. Al plate electrodes (99.2% purity) were used in the batch reactor with 5 cm apart without adjusting their pH (i.e., initial pH 6.2). In every experiment, the anode and cathode were submerged (95% of surface area) in wastewater. To

construct the electrodes, i.e., anode and cathode, two identical pieces of 0.5 mm-thick Al plates were cut into 10 cm in length and 4 cm in width. Prior to every study, any oxide layer on the electrode's surface should be removed using sandpaper with a grit level of 200. The parameters of ECP [fixed current density = 50 mA/cm^2, electrode distance = 5 cm, electrode combination = X-anode/X-cathode (where X= Al, Fe, Cu, and Zn), reaction time = 60 min] were applied by using a DC power supply arranged in monopolar parallel configuration. Whatman filter paper no.2 (diameter 110 mm) was used to filter the reactor's effluent during each study. Metal ions dissolve at the Al plate (anode) while hydroxyl ions and H_2 are formed at the cathode (**Fig. S2**).

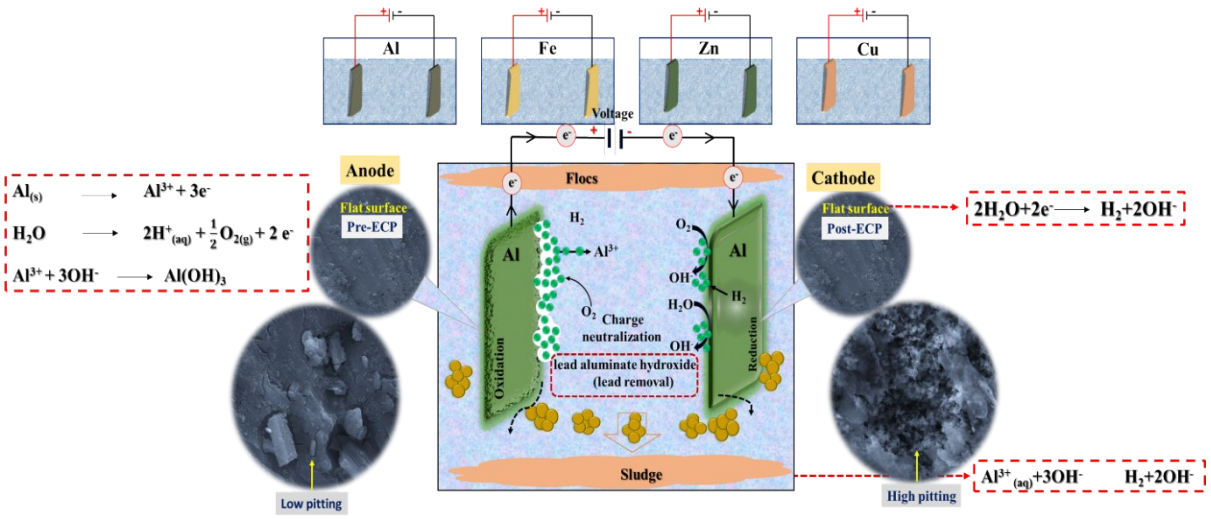

Fig. S2 Schematic representation of the textile wastewater treatment by different metal electrodes and its mechanism using an Al electrode as anode and cathode.

During ECP, electrolytic reactions occurred and caused coagulants in the aqueous solution. These coagulants are then produced by adsorption, surface complexation, or electrostatic attraction, trapping contaminants onto the surface, and causing the organic pollutants to gather. H_2 bubbles produced during this process cause flotation. Additionally, in the stability study, a challenging task was carried out, such as pre- and post-investigations, with ease. The effluent treatment under an electrochemical reactor was studied in batch

reactor mode by galvanostatic under ambient conditions. Herein, the sample was diluted using deionized water, and then the concentration of Pb^{2+} ions was analyzed by AAS.

Table S2 The detailed mechanism during ECP by respective electrodes such as Al, Fe, Cu, and Zn.

S.No	Electrode	Anode	Cathode	Overall
1.	Fe	$Fe_{(s)} \rightarrow Fe^{2+}_{(aq)} + 2e^-$ $Fe^{2+}_{(aq)} + 2OH^- \rightarrow Fe(OH)_{2(s)}$ Or $Fe_{(s)} \rightarrow Fe^{3+}_{(aq)} + 3e^-$ $Fe^{3+}_{(aq)} + 3OH^-_{(aq)} \rightarrow Fe(OH)_{2(s)}$	$2H_2O_{(l)} + 2e^- \rightarrow H_{2(g)} + 2OH^-_{(aq)}$ $3H_2O_{(l)} + 3e^- \rightarrow \frac{3}{2}H_{2(g)} + 3OH^-_{(aq)}$	$Fe^{2+}_{(s)} + H_2O_{(l)} \rightarrow Fe(OH)^{2}_{(}$ $Fe^{2+}_{(s)} + H_2O_{(l)} \rightarrow FeOH_{(3)}$
2.	Al	$Al_{(s)} \rightarrow Al^{3+}_{(aq)} + 3e^-$	$3H_2O_{(l)} + 3e^- \rightarrow \frac{3}{2}H_{2(g)} + 3OH^-_{(aq)}$	$Al^{3+}_{(s)} + 3H_2O_{(l)} \rightarrow AlOH_{(3)}$
3.	Cu	$Cu_{(s)} \rightarrow Cu^{2+}_{(aq)} + 2e^-$	$2H_2O_{(l)} + 2e^- \rightarrow H_{2(g)} + 2OH^-_{(aq)}$	$2Cu_{(s)} + 3H_2O_{(l)} + \frac{1}{2}O_2(g) \rightarrow$
4.	Zn	$Zn_{(s)} \rightarrow Zn^{2+}_{(aq)} + 2e^-$	$2H_2O_{(l)} + 2e^- \rightarrow H_{2(g)} + 2OH^-_{(aq)}$	$Zn^{2+} + 2OH^- \rightarrow Zn(OH)_2$

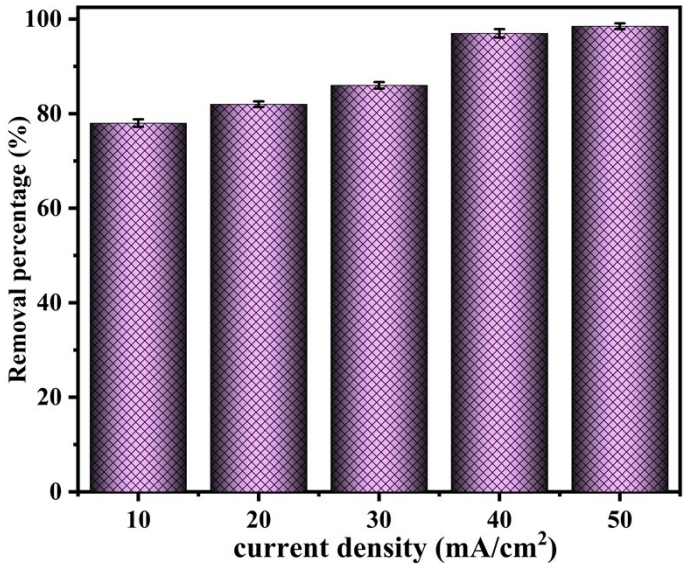

Fig. S3 Removal efficiency percentage bar graph for various current densities (electrode combination– Al/Al, electrode distance – 5 cm, pH 5, and reaction time 60 min).

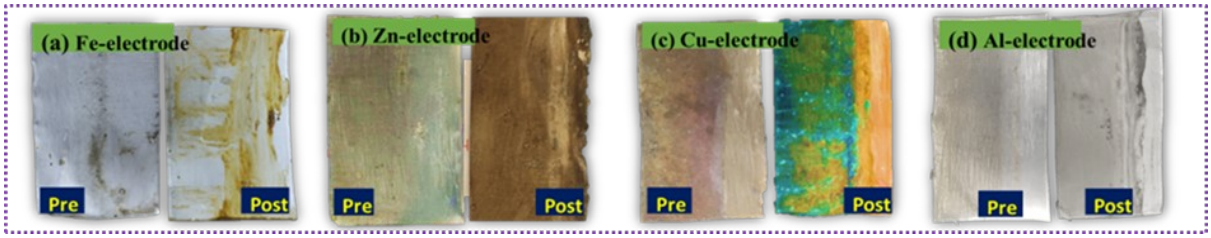

Fig. S4 Various electrode photographs of pre- and post-ECP studies. **(a)** Fe electrode **(b),** Zn electrode **(c),** Cu electrode, and **(d)** Al electrode.

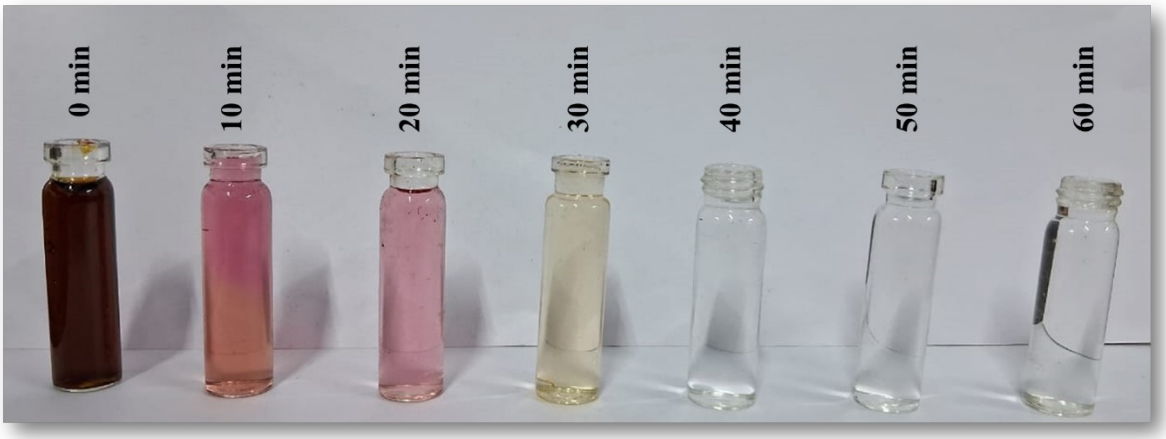

Fig. S5 Photographs of effluent before (intense and dark) and after (bleaching) ECP at operating conditions (operating conditions: electrode combination– Al/Al, electrode distance – 5 cm, pH 5, and reaction time 60 min).

Table S3 Textile effluent degradation process carried out using Al-ECP concerning TOC, TC, IC, and the corresponding percentage degradation.

S. No	Time (min)	Experimental values for Al-ECP		
		TOC (mg/L)	IC (mg/L)	TC (mg/L)
1.	0	307.80	1050.00	1360.00
2.	10	60.95	80.76	150.71
3.	20	60.21	160.84	230.04
4.	30	40.71	130.48	180.18
5.	40	40.51	130.77	180.27
6.	50	40.42	120.64	170.06
7.	**60**	**30.29**	**130.21**	**160.05**

Table S4 Textile effluent degradation process carried out using the Fe-ECP concerning TOC, TC, IC, and the corresponding percentage degradation.

S. No	Time (min)	Experimental values for Fe-ECP		
		TOC (mg/L)	IC (mg/L)	TC (mg/L)
1.	0	307.8	1050.00	1360.00
2.	10	80.71	250.93	340.64
3.	20	70.00	260.64	330.64
4.	30	50.22	310.85	370.07
5.	40	40.58	370.89	420.48
6.	50	36.79	370.36	333.57
7.	**60**	**30.96**	**400.40**	**440.36**

Table S5 Textile effluent degradation process carried out using the Cu-ECP concerning TOC, TC, IC, and the corresponding percentage degradation.

S. No	Time (min)	Experimental values for Cu-ECP		
		TOC (mg/L)	IC (mg/L)	TC (mg/L)
1.	0	307.8	1050.00	1360.00
2.	10	80.30	290.47	370.77
3.	20	80.01	240.11	320.12
4.	30	70.65	260.91	340.56
5.	40	70.00	260.64	330.64
6.	50	60.42	250.58	320.01
7.	**60**	**60.36**	**360.25**	**420.61**

Table S6 Textile effluent degradation process carried out using the Zn-ECP concerning TOC, TC, IC, and the corresponding percentage degradation.

S. No	Time (min)	Experimental values for Zn-ECP		
		TOC (mg/L)	**IC (mg/L)**	**TC (mg/L)**
1.	0	307.8	1050.00	1360.00
2.	10	90.84	150.70	250.53
3.	20	90.00	300.78	390.77
4.	30	80.23	220.73	300.96
5.	40	80.18	250.25	330.43
6.	50	70.87	160.05	230.92
7.	**60**	**70.48**	**190.89**	**270.37**

Table S7 EIS-derived R_s and R_{ct} for different electrodes.

Electrodes	R_s (Ω)	R_{ct} (Ω)
Al	**12.2**	**5.33**
Fe	15.6	90.4
Cu	18.5	150.5
Zn	39.6	164.4

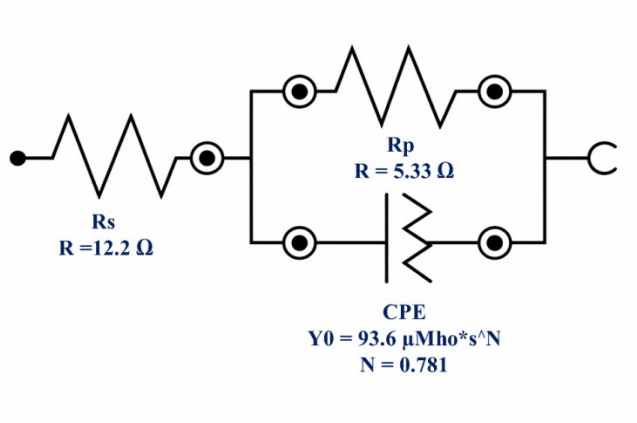

Fig. S6 Equivalent circuit fitted result of the Al electrode.

SI3. Electrode stability and corrosion behaviour in electrocoagulation

Among the evaluated electrode materials such as Al, Fe, Zn, and Cu, the Al electrode performance remains good during the ECP. Al electrode maintained stable operating conditions throughout the study and demonstrated consistent pollutant removal effectiveness. The enhanced stability can be attributed to the controlled dissolving behaviour of Al during the ECP, which supports the continual generation of aluminum hydroxide [$Al(OH)_3$] species that serve as efficient coagulants for pollutant removal. Other electrode materials such as Fe, Cu, and Zn, demonstrated significantly less operational stability under the identical conditions. Fe electrodes oxidize quickly and generate dense oxide layers, which leads to a decrease in the process's efficiency over time. Similarly, Zn and Cu electrodes are more susceptible to corrosion and surface passivation during electrochemical processes, limiting their long-term efficiency and stability in wastewater treatment applications. Based on these

observations, the findings of this study show that the Al electrodes possess higher operational stability and lower corrosion susceptibility than the Fe, Zn, and Cu electrodes under the investigated conditions.

Further, the Pilling-Bedworth rule states that aluminum electrodes are more resistant to corrosion due to the production of a dense and adherent oxide layer (Al_2O_3) on their surface. This passive oxide layer serves as a protective barrier, limiting additional oxidation and preventing rapid degradation of the electrode surface. The Al electrode has a good oxide volume-to-metal volume ratio, allowing the oxide coating to efficiently cover the metal surface and minimize corrosion. As a result, the Al electrode has higher corrosion resistance than other electrode materials like Fe, Zn, and Cu. While the results show promising treatment performance, additional research is required to integrate the long-term operation with scale-up evaluation to give a more complete assessment of electrode durability and process efficiency. Colour, TOC, and heavy metal analysis, as well as pre- and post-studies of electrode surface interpretation are the major tasks in industrial wastewater treatment, indicating its physicochemical properties. Post-ECP was thoroughly studied using FE-SEM, FT-IR, electrochemical tools, and sludge using XPS.

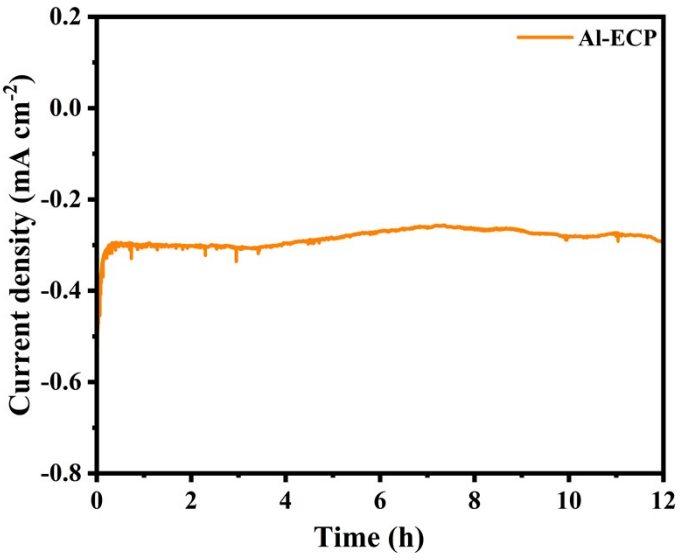

Fig. S7 CA profile of long-term stability study of the Al electrode after using five cycles.

SI4. Faradaic Efficiency (FE) measurements

Quantifying aluminum mass loss and reporting faradic efficiency would provide a clearer understanding of electrode consumption and the long-term feasibility of the ECP. To determine the mass loss of aluminum during operation, further studies were conducted. The electrodes were weighed before (initially at 0 min – pristine Al electrode) and after (After 60 min ECP (3600 sec)) cycle using a precision analytical balance (± 0.1 mg accuracy), under optimum conditions [current density – 50 mA/cm^2, electrode distance – 5 cm, pH – 2, electrolysis time – 60 min].

Furthermore, the theoretical aluminum dissolution was calculated based on Faraday's law:

$$m = \frac{I \times t \times M}{z \times F}$$

Where m is the theoretical mass dissolved, I is current (A), t is time (s), M is the molar mass of Al (26.98 g/mol), z = 3(for Al^{3+}), and F is Faraday's constant (96485 C/mol)

$$m = \frac{0.05 \times 3600 \times 26.98}{3 \times 96485}$$

$$m = \frac{4856.4}{289455} = 0.01678 \text{ gm}$$

Experimental mass loss,

$$m_{exp} = W_{initial} - W_{final}$$

Where $W_{initial} = 5.3739$, $W_{final} = 5.3601$

$$m_{exp} = 5.3739 - 5.3601 = 0.0138 \text{ gm}$$

$$Faradaic\ efficiency\ (FE\%) = \frac{m_{exp}}{m_{theo}} \times 100 = \frac{0.01380}{0.01678} \times 100$$

(FE %) = 82.24 %

Under the applied current of 0.05 A (50 mA/cm^2) and an electrolysis time of 3600 s (60 min), the experimentally measured aluminum mass loss was 0.0138 gm. The theoretical aluminum dissolution was calculated using Faraday's law, which predicts a value of 0.0168 g under the same operating conditions. By comparing the experimental and theoretical values, the faradaic efficiency was determined to be approximately 82.24 %, indicating that the majority of the applied current contributed to the anodic dissolution of aluminum with limited parasitic reactions.[1] These results have confirmed that controlled electrode consumption supports the stability and practical feasibility of the aluminum electrode in the ECP.

SI5. As the current density increased, the pits got deeper and wider

Fig. S8a-f depicts anodic pit-growth for an increasing current density, following ECP treatment at varying applied current densities, as proven by the optical microscope. Optical microscope images of the Al electrode surfaces were obtained. The surface morphology of the Al electrode exhibited increasingly wider and deeper pits as the applied current density increased, indicating enhanced anodic dissolution and specific corrosion activity. Before ECP, optical images of the anode surface were visually verified with no pits, as shown in **Fig S8a**. In the post-treatment study, the Al electrode at 10 mA/cm^2 exhibited initial surface roughness and the appearance of small pits resulting from localized anodic dissolution. When applied current densities increased from 20 to 40 mA/cm^2, the surface shows enhanced corrosion traits, characterized by deeper pits and increased roughness. While current density increased to 50 mA/cm^2, major degradation on the electrode surface is evident, characterized by widespread etching, breakdown, and deep structural deformation, confirming intensive anodic activity at high current densities.

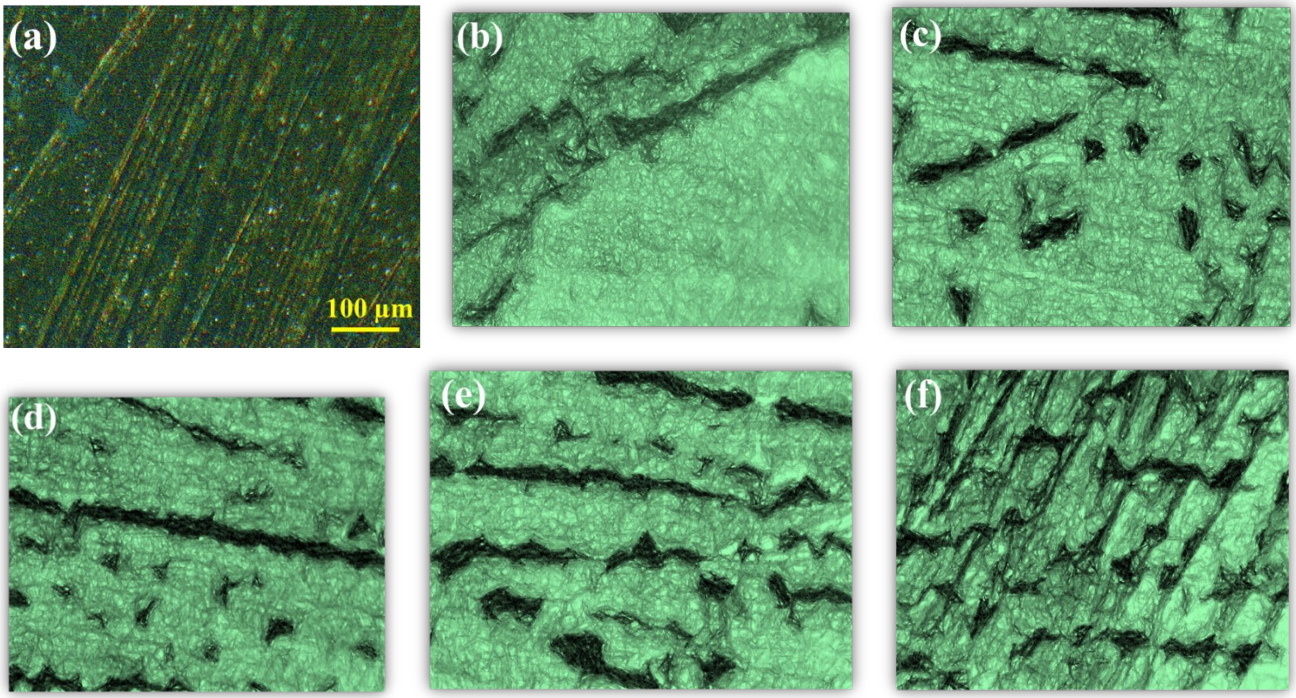

Fig. S8 Optical microscopic images of pre-studied cathode surface of Al-ECP **(a)** and post-studied cathode surface of Al-ECP at different CD 10, 20, 30, 40, and 50 mA/cm^2 **(b-f)**.

SI6. Bacterial strain and culture conditions

Escherichia coli (*E.coli*) was used as the model bacterial strain. The culture was grown in nutrient broth at 35-37 °C with continuous shaking at 150 rpm for 15–18 h. Cells were harvested by centrifugation at 5000 rpm for 10 min, and the resulting pellet was washed thrice with distilled water to remove the residual medium components.

SI6.1 Preparation of bacterial suspension and treatment. The washed bacterial suspension was diluted with treated and untreated water samples to obtain a uniform bacterial suspension.

SI6.2 Enumeration of viable bacteria. The bacterial concentration was determined using the standard plate count method. Briefly, 100 µL aliquots from ten-fold serial dilutions of the suspension were spread on nutrient agar plates. The plates were incubated at 37 °C for 18 h, and the colonies were enumerated. The obtained results were expressed as colony-forming units per millilitre (CFU/mL).

Economic Feasibility

The energy consumption (Q), electrode consumption (W), disposal charge (D), and operating cost (M) for the ECP units were calculated in **Eqns (S4-S7)**.[2]

$$Q = U \times I \times t \times \frac{c}{q} \quad \textbf{(S4)}$$

$$W = m \times \frac{p}{q} \quad \textbf{(S5)}$$

$$D = a \times b \quad \textbf{(S6)}$$

$$M = Q + W \quad \textbf{(S7)}$$

Where U stands for voltage (V), I for current (A), t for operation time (h), and c for the average energy cost in US ($/m^3). q for water volume (m^3/d), a is stands for flocs per volume of treated water generated in ECP (kg/m^3), and b is the disposal fee of solid water per kilogram of waste ($/kg).

References

1 K. Mansouri, K. Ibrik, N. Bensalah, A. Abdel-Wahab, Anodic dissolution of pure aluminum during electrocoagulation process: Influence of supporting electrolyte, initial pH, and current density, *ACS Ind. Eng. Chem. Res.* 2011, **50**, 13362–13372.

2 R. Shah, D. Eldridge, E. Palombo, and I. Harding, Optimization and stability assessment of solid lipid nanoparticles using particle size and zeta potential, *J. Phys. Sci.* 2014, **25**, 59–75.